

Host isotope effects on midinfrared optical transitions in silicon

Gordon Davies,* S. Hayama, and Shiqiang Hao

Department of Physics, King's College London, Strand, London WC2R 2LS, United Kingdom

B. Bech Nielsen

Institute of Physics & Astronomy, University of Aarhus, DK-8000 Aarhus C, Denmark

J. Coutinho

Department of Physics, University of Aveiro, Campus Santiago, 3810 Aveiro, Portugal

M. Sanati and S. K. Estreicher

Department of Physics, Texas Tech University, Lubbock, Texas 79409-1051, USA

K. M. Itoh

Department of Applied Physics and Physico-Informatics, Keio University, Yokohama 223-8522, Japan

(Received 11 November 2004; revised manuscript received 4 January 2005; published 29 March 2005)

The effects of changing the host-lattice isotopes from natural silicon (approximately ^{28}Si) to ^{30}Si are reported for some of the important local vibrational modes (LVMS) observed in as-grown and electron-irradiated Czochralski silicon. We show that the quanta of the LVMS shift to lower energy in ^{30}Si compared to natural silicon by amounts varying from 3.5 to 27 cm^{-1} , in very good agreement with predictions from density functional theory. The 2767 cm^{-1} ("3.6 μm ") transition of the negative divacancy is also found to shift to lower energy with increasing silicon mass, but we demonstrate, using an empirical method of predicting the shifts of zero-phonon lines, that the line is a zero-phonon line. The empirical method used is verified by analyzing the shifts of the very-low energy 3942 cm^{-1} vibronic band.

DOI: 10.1103/PhysRevB.71.115212

PACS number(s): 78.30.Am, 31.30.Gs, 63.20.Pw

I. INTRODUCTION

Currently there is considerable interest in studying the effects on optical transitions in silicon of changing the isotopes of the host lattice. Studies have been made on Raman scattering from isotope superlattices,¹ on the indirect energy gap,² and on the electronic states of the shallow donors and acceptors.³⁻⁶ Many of the deep centers created by radiation damage and ion implantation which produce photoluminescence in the near infrared spectral range ($>6000 \text{ cm}^{-1}$) have also been investigated.^{7,8} To date, the only measurements made on local vibrational modes have been on interstitial oxygen⁹ and bond-centered hydrogen.¹⁰

In Sec. III of this paper we present experimental data and quantitative analyses of the isotope dependence of some of the most common local vibrational modes observed in as-grown and electron-irradiated Czochralski silicon. We report that the vibrational modes of substitutional carbon, interstitial oxygen, carbon-oxygen complexes, and the vacancy-oxygen A center shift to lower energy in ^{30}Si compared to natural silicon, by amounts varying from 3.5 to 27 cm^{-1} . We show that the measured shifts are in very close agreement with predictions from current density functional theory. In Sec. IV we observe that the 2767 cm^{-1} transition of the negative divacancy also shifts to lower energy with increasing silicon mass. This behavior is the opposite of the shifts for all known zero-phonon lines in silicon, and, together with the very large width of the line, would be consistent with the involvement of a phonon in the transition. We verify that an

empirical method of predicting the zero-phonon shifts works for a known very-low energy vibronic band, and we use that method to confirm that the 2767 cm^{-1} line is indeed a zero-phonon line.

We begin by describing the experimental arrangements (Sec. II).

II. TECHNICAL DETAILS

The isotopically enriched Czochralski ^{30}Si sample used here¹¹ had a mean mass number of $\bar{M}(^{30}\text{Si})=29.98$, derived from Secondary Ion Mass Spectroscopy (SIMS) measurements of the isotope content as 98.74% ^{30}Si , 0.59% ^{29}Si , and 0.67% ^{28}Si . We confirm $\bar{M}(^{30}\text{Si})$ from the optical measurements in Sec. III. Using standard calibrations,¹² the ^{30}Si sample was found to contain $3 \times 10^{17} \text{ cm}^{-3}$ substitutional carbon and $8.8 \times 10^{17} \text{ cm}^{-3}$ interstitial oxygen. Shallow dopants, mainly substitutional boron at $[B]=5.5 \times 10^{16} \text{ cm}^{-3}$, were of negligible concentrations since the sample was irradiated, at nominal room temperature, with 1.5 MeV electrons to a dose of $5 \times 10^{17} \text{ cm}^{-2}$. Comparisons have been made with electron-irradiated Czochralski samples of normal isotope content and of similar ^{16}O and ^{12}C or ^{13}C content. The absorption measurements were made with the samples at 8 K on the cold-finger of a closed cycle cryostat, using a Nicolet Fourier transform spectrometer fitted with a KBr beamsplitter and an MCT detector cooled to 77 K. The resolution, as given by the full width at half height of residual atmospheric absorption was 0.5 cm^{-1} .

We refer to samples with the normal isotope content as “natural silicon.” Throughout, values of wavenumbers quoted without qualification are for natural silicon, ^{16}O , and ^{12}C in the limit of low temperature.

Local vibrational modes of the centers considered here have been investigated by first principles calculations, usually for natural silicon, and the calculations have been repeated for ^{30}Si . Dynamical matrix elements were evaluated using linear response theory,¹³ or by explicitly displacing the impurities and its Si neighbors along all Cartesian coordinates.¹⁴ Further details of the methods are given below where they are used, together with the laboratory implementing them.

III. VIBRATIONAL TRANSITIONS

Silicon produces appreciable optical absorption in the region 500 to 1450 cm^{-1} by creating two and three phonons. This intrinsic absorption has been removed from the spectra by subtracting the absorption spectrum of a natural float-zone reference sample of high purity. For the ^{30}Si spectra, the frequency scale of the reference spectrum must be reduced to allow for the mass change. We assume that the vibrations are harmonic. Then, changing the mass simply changes the vibrational frequency in the inverse ratio of the square root of the effective masses. A small mismatch in the frequency scales shows itself by producing highly visible “derivative type” features in the difference spectrum, and removing them is very sensitive to the assumed mass. To fit the natural spectrum to the ^{30}Si spectrum requires the ^{30}Si sample to have a mean mass of 29.96 ± 0.01 (in the harmonic approximation), in very close agreement with the SIMS analysis, Sec. II. Difference spectra in the region of the strongest intrinsic two-phonon absorption in silicon are shown in Fig. 1. Isotope shifts of the local vibration modes of substitutional carbon are clearly observable.

For vibrations involving impurities, the change in the effective mass is determined by the specific mode being considered. In addition, isotope effects occur through the anharmonic part of the potential by two processes. First, the anharmonicity of all the modes of vibration of the crystal result in a change in lattice parameter with isotope mass. The change between natural silicon and ^{30}Si has been measured at low temperature^{15,16} as $\Delta V/V = -1.68(2) \times 10^{-4}$. The change in frequency ω with volume V is represented by the Grüneisen parameter $\gamma = -d(\ln \omega)/d(\ln V)$. Typically $|\gamma| \approx 1$ for lattice modes in silicon,¹⁷ and in the limit of low volume change $\gamma = 0.2$ for the local vibrational mode at 1136 cm^{-1} of interstitial oxygen.¹⁸ For a value of $|\gamma| = 1$, the volume change would produce a change of only $\pm 0.2 \text{ cm}^{-1}$ for a mode of quantum 1000 cm^{-1} . This change is little more than the uncertainty in measuring the peak positions, and is more than an order of magnitude smaller than the shifts reported below.

A second effect of anharmonicity comes from the local vibrational mode itself. This effect can be illustrated by introducing a cubic potential term bQ^3 to the harmonic potential $\frac{1}{2}m\omega^2Q^2$ for an effective mass m vibrating at angular frequency ω in a coordinate Q . For example, the cubic term

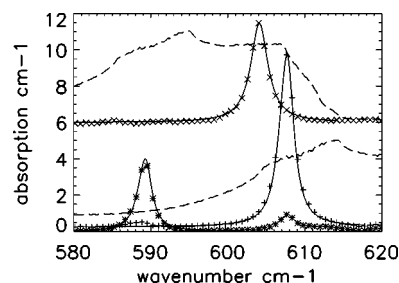


FIG. 1. Absorption produced by the LVM of carbon. The broken line in the lower figure shows the absorption spectrum of a pure float-zone $^{\text{nat}}\text{Si}$ sample. The absorption spectrum of a $^{\text{nat}}\text{Si}$ sample doped with ^{13}C , after removal of the intrinsic absorption, is shown by asterisks. The peak at 589 cm^{-1} is from ^{13}C , and that at 607 cm^{-1} from trace ^{12}C in the same sample. Points + show the absorption measured in a $^{\text{nat}}\text{Si}$ sample doped with ^{12}C . The lines through the points for the 589 and 607 cm^{-1} peaks are fits as described in Sec. III A, allowing for the random isotope distribution. The upper part of the figure shows spectra for ^{30}Si . The broken line shows the intrinsic lattice absorption in ^{30}Si as calculated by scaling the frequency axis of an absorption spectrum of the float-zone sample. Points \times show the absorption produced by ^{12}C in that sample after removing the intrinsic absorption. The line through the 604 cm^{-1} peak is the fit of a single Lorentzian. For clarity, only representative experimental points are shown, and the ^{30}Si data have been displaced vertically by 6 cm^{-1} .

b can be adjusted so the transition energy between the zeroth and first vibrational states is 10% lower than the transition energy in the unperturbed harmonic oscillator. Then, a change in the effective mass from 28 to 30 units produces a change in transition energy that would be the same, within our experimental uncertainties, to the change predicted if the mode was assumed to be harmonic.

These estimates show that the contributions of the anharmonic terms in the potential to the host isotope effects are very small. The shifts expected on changing the isotope will derive primarily from the simple result that for a harmonic potential, the vibrational frequency is inversely proportional to the square root of the effective mass. This result is important, since it allows us to make a direct comparison between experiment and the *ab initio* calculations, which employ a harmonic formalism.

A. Substitutional carbon

The vibrational frequency of substitutional carbon, C_s , is 607.5 cm^{-1} in natural silicon, only $\sim 15\%$ higher than the maximum mode frequency (525 cm^{-1}) of silicon. If the vibration only involved Si atoms, the mode would experience an isotope shift of $\sim -19 \text{ cm}^{-1}$ between ^{30}Si and $^{\text{nat}}\text{Si}$. The observed shift is only -3.5 cm^{-1} . The vibrational frequency of C_s in ^{28}Si has been predicted to be 598 cm^{-1} using a 64-atom supercell with the local density approximation in the SIESTA code at Texas Tech.^{13,19} Adapting the dynamical matrix for ^{30}Si gives 593.6 cm^{-1} , a shift of -4.6 cm^{-1} in close agreement with experiment.

Since changing the silicon isotopes produces only a small shift, the random assembly of isotopes in natural silicon may

broaden and shift the optical transition relative to single-isotope material. It is useful to know the size of these effects. If only one nearest-neighbor Si atom is ^{30}Si , and the other three are ^{28}Si , the local vibrational mode (LVM) will be split in the trigonal symmetry; the SIESTA code predicts shifts of -1.0 cm^{-1} for the doublet and -1.9 cm^{-1} for the singlet. The splitting is sufficiently small that the doublet and singlet may be represented by a single peak at their weighted mean, which is very close to one quarter of the total shift for complete isotope substitution. We assume that n ^{30}Si atoms in the nearest neighbor positions produce n times the shift of one atom, and that each ^{29}Si atom produces half the shift of a ^{30}Si atom. Since our calculations overestimate the shifts, for a comparison with experiment we scale our shifts by a factor of 3.5/4.6. With these simple assumptions and using random populations of Si isotopes on the four nearest-neighbor sites to each C atom, we fit the line shape of the carbon LVM. First, we take the line shape as measured with ^{13}C in $^{\text{nat}}\text{Si}$, Fig. 1. The line shape is reproduced when the Lorentzian component curves have full widths at half-height of $1.9\pm 0.1\text{ cm}^{-1}$, compared to the measured linewidth of $2.2\pm 0.1\text{ cm}^{-1}$; the lattice isotope effect contributes $\sim 0.3\text{ cm}^{-1}$ to the width. The random isotopes leave the line shape still closely symmetric, and the calculation suggests that in ^{28}Si the peak of the LVM would be about 0.15 cm^{-1} to higher energy than in the $^{\text{nat}}\text{Si}$ used here, marginally improving the agreement with theory but close to the experimental accuracy.

We have first fitted the LVM of ^{13}C since its energy is well below the strong two-phonon absorption band between 600 and 630 cm^{-1} , Fig. 1. The LVM of ^{12}C in $^{\text{nat}}\text{Si}$ is superimposed on the low energy part of the band, Fig. 1, and in our sample can be reproduced, just like the ^{13}C line, by a sum of Lorentzians with the same widths of $2.0\pm 0.1\text{ cm}^{-1}$. Moving to ^{12}C in *single-isotope* ^{30}Si places the LVM on the high-energy part of the two-phonon band, Fig. 1. The width is $2.7\pm 0.1\text{ cm}^{-1}$, some $35\pm 20\%$ larger than each Lorentzian component in the Si samples, even though there is now no random isotope content. The absorption spectra confirm that the temperature of the sample was $\sim 10\text{ K}$, and the width of the zero-phonon lines observed at this sample show that the increased width is not caused by severe strain in the crystal. One contribution to the linewidth is the broadening produced by the decay of the LVM into two phonons, which depends partly on the density of two-phonon states at the energy of the LVM. The density of two-phonon states has been calculated from the one-phonon density of states given by Pavone *et al.*²⁰ We find that the two-phonon density increases by 70% between 589 cm^{-1} in $^{\text{nat}}\text{Si}$ and 604 cm^{-1} in ^{30}Si . The increasing number of decay channels may be partly responsible for the increased linewidth.

B. Interstitial oxygen

Lattice isotope effects on interstitial oxygen have been reported in detail by Kato *et al.*⁹ All our data agree to within 0.2 cm^{-1} . We also report the shift of the 518.3 cm^{-1} line as -16.9 cm^{-1} from natural silicon to ^{30}Si .

Calculations have been made using density functional

theory implemented at King's College London by the VASP package on a 64-atom supercell.²¹ The 1136 cm^{-1} mode is predicted²¹ to shift by -7.1 cm^{-1} , in close agreement with the observed -7.3 cm^{-1} . We recall that the volume change will give a further small shift of -0.04 cm^{-1} , Sec. III. By considering ^{28}Si atoms in the nearest-neighbor positions relative to the O atom, and placing ^{30}Si atoms in the six next-nearest positions, the VASP calculations give a shift of only -0.04 cm^{-1} ; that is, the isotope shift occurs primarily from the effect of the nearest neighbor atoms. This is confirmed by noting that in $^{\text{nat}}\text{Si}$, the $^{30}\text{Si}-^{16}\text{O}-^{30}\text{Si}$ configuration occurs at the same energy, within experimental uncertainties, as we find in our all- ^{30}Si crystal.²²

The 518 cm^{-1} mode, resonant with the lattice vibrations, is predicted to involve almost entirely the motion of the neighboring Si atoms, and so the observed isotope shift of -16.9 cm^{-1} is very close to that expected for an all-Si mode, -18.2 cm^{-1} .

An A_{1g} symmetric stretch is predicted, but has not been observed,²² at 600 cm^{-1} . We calculate that it will shift by -19.6 cm^{-1} . If the 1748.8 cm^{-1} line is a combination of the 1136 and 600 cm^{-1} vibrations, the combination would have a total shift of -26.7 cm^{-1} in the harmonic approximation, in close agreement with the measured -27.4 cm^{-1} , and providing confirmation for that assignment.

C. Interstitial carbon and complexes

Data are gathered in Table I for the measured isotope effects on the interstitial carbon atom, C_i , the interstitial-carbon plus self-interstitial, $C_i\text{-Si}_i$, the "C3" interstitial-carbon plus interstitial-oxygen, $C_i\text{-O}_i$, and the "C4" interstitial-carbon plus interstitial-oxygen and self-interstitial, $C_i\text{-O}_i\text{-Si}_i$.

The interstitial carbon atom C_i is generated by radiation damage, when a self-interstitial is captured by a substitutional C atom; C_i is stable up to room temperature, and so it may be created by irradiating and storing the sample at $T < 300\text{ K}$. It produces two absorption lines²³ at 932.3 and 922.3 cm^{-1} . In ^{30}Si , we observe the lines at 924.4 and 916.8 cm^{-1} ; positive identification that they are produced by C_i comes from the intensity ratio of the lines, and their disappearance from the spectrum on annealing at room temperature. The frequencies and isotope shifts calculated in Aveiro using a supercell density functional code, AIMPRO,¹⁴ agree well with experiment, although the predicted isotope shifts agree better when transposed (Table I). The ^{30}Si data complete the set of isotope data for this center: with ^{13}C doping, the lines are known²⁴ to be at 892 and 904 cm^{-1} , showing that they are predominantly vibrations of C.

A defect assigned²⁵ to an interstitial-carbon plus a self-interstitial produces LVM lines at 966.7 and 960.3 cm^{-1} . There appear to be no other isotope data available for this center, and we have not calculated its properties.

Radiation damage creates the well-known "C3" complex when an interstitial carbon atom is trapped by an interstitial oxygen atom,²⁶ producing a structure in which the C and O atoms are at opposite corners of an approximately square complex, with the other two corners occupied by Si atoms.²⁷

TABLE I. Measured (8 K) and calculated host-isotopic shifts. In this table, carbon refers to ^{12}C . The column “Si-only” gives the shift if only Si atoms were involved in the vibration, and the results from the *ab initio* density functional calculations are given as the “Calculation.” The values calculated for the COV and V_2 centers are by the empirical methods of Sec. IV A and IV B.

| Center | $^{\text{nat}}\text{Si}$ (cm^{-1}) | Experiment ^{30}Si (cm^{-1}) | Shift (cm^{-1}) | Calculation (cm^{-1}) | Si only (cm^{-1}) |
|--------------------------|--|--|-------------------------------|-------------------------------------|---------------------------------|
| C_s | 607.5 | 604.0 | -3.5 | -4.6 | -19.3 |
| O_i | 518.3 | 501.4 | -16.9 | ~ -18 | -18.2 |
| | 1136.4 | 1129.1 | -7.3 | -7.1 | -36.0 |
| | 1205.7 | 1197.3 | -8.4 | | -38.2 |
| | 1748.8 | 1721.4 | -27.4 | -26.7 | -55.4 |
| | | | | | |
| C_i | 922.3 | 916.8 | -5.5 | -8.3 | -29.2 |
| | 932.3 | 924.4 | -7.9 | -5.7 | -29.5 |
| $\text{C}_i\text{-Si}_i$ | 966.7 | 961.8 | -5.9 | | -30.6 |
| | 960.3 | 952.4 | -7.9 | | -30.4 |
| C3 | 529.6 | 515.4 | -14.2 | -14.2 | -16.8 |
| | 549.9 | 532.2 | -17.7 | -18.5 | -17.4 |
| | 588 | 569 | -19 | -17.4 | -18.6 |
| | 742.8 | | | -4.2 | -23.5 |
| | 865.9 | 857.8 | -8.1 | -8.1 | -27.4 |
| C4 | 1116.3 | 1111.5 | -4.8 | -5.0 | -35.4 |
| | 939.8 | 933.2 | -6.6 | -5.3 | -29.8 |
| VO | 1024.2 | 1017.5 | -6.7 | -6.8 | -32.5 |
| | 835.7 | 829.8 | -5.9 | -6.4 | -26.5 |
| COV | 3942.1 | 3943.6 | +1.5 | (+3) | |
| V_2 | 2767 | 2764.2 | -2.8 | (-2.4) | |

Six LVMs are known from experiment,²⁸ and are listed in Table I. This table extends the isotope shifts reported in Ref. 7, where only the two LVMs that are easily visible in the photoluminescence spectrum were given. Table I lists also the frequencies calculated in Aveiro using AIMPRO. Again, the agreement is excellent. Combined with the data obtained from the same optical center by photoluminescence,⁷ the silicon isotope shifts have now been measured for 5 modes of this center, with an average agreement between theory and experiment of better than 4%. For completeness, we note that the effects of changing the oxygen and silicon isotopes are largely known.^{25,28,29}

With increasing radiation doses, the “C3” $\text{C}_i\text{-O}_i$ center acts as a nucleation center for capturing self-interstitials,²⁶ forming first the “C4” $\text{C}_i\text{-O}_i\text{-Si}_i$ complex. This center produces two known LVM lines²⁸ at 939.8 and 1024.2 cm^{-1} , which we find move to 933.2 and 1017.5 cm^{-1} , respectively, in ^{30}Si ; both lines move by -6.6 cm^{-1} , compared to shifts of -30 cm^{-1} if the vibrations were all silicon. We find that in ^{13}C -doped natural silicon, the lines move, respectively, to 911.2 and 1012.5 cm^{-1} . For completeness, Murin reports²⁴ that on changing from ^{16}O to ^{18}O (with ^{12}C and $^{\text{nat}}\text{Si}$), the lines move to 939.2 and 982.3 cm^{-1} : the first mode predominantly involves motion of the C atom, and the second predominantly the O atom. *Ab initio* calculations using again the methods of Ref. 14 have been used to investigate the reaction between $\text{C}_i\text{-O}_i$ and a Si self-interstitial (Si_i). The ground state of the C4 complex was found to be similar to the O

form of $\text{C}_i\text{-O}_i\text{-H}$ (see Fig. 4 in Ref. 14), with the Si_i atom taking the place of the H atom. In this structure the Si_i atom is directly bound to C, producing a strong Si-C bond, of length 1.84 Å, along $[\bar{1}01]$, similar to the $\sim 1.88 \text{ Å}$ nearest-neighbor distance in SiC crystals. The $^{12}\text{C}_i\text{-}^{12}\text{O}_i\text{-}^{28}\text{Si}_i$ complex is predicted to produce at least four local vibrational modes at 998.4, 908.3, 744.4, and 682.7 cm^{-1} . The two higher frequencies underestimate the 1024.2 and 939.8 cm^{-1} absorption frequencies by only about 30 cm^{-1} . The four modes are mostly localized at the O and C impurities, and represent, respectively, the asymmetric stretching of the Si-O-Si unit, a mode analogous to the high-frequency of C_i , a mode analogous to the low frequency mode of C_i , and a stretch mode at the $\text{Si}_i\text{-C}$ unit along $[\bar{1}01]$. Additional modes at lower frequencies are also predicted. However, these should be difficult to detect as they involve the motion of strained Si bonds or the symmetric stretch motion of the Si-O-Si unit. We calculate that the predicted 998.4 cm^{-1} mode shifts by -44.0 and -8.3 cm^{-1} for ^{18}O and ^{13}C substitutions, respectively, in fair agreement with the measured -41.9 and -11.7 cm^{-1} , Ref. 24. Under the same conditions, the 908.3 cm^{-1} mode shifts downwards by -0.4 and -29.1 cm^{-1} , again in agreement with the measured -0.6 and -28.6 cm^{-1} shifts, respectively. The ^{30}Si shifts are reported and compared to our measurements in Table I. For these modes, the calculations give shifts of -6.8 and -5.3 cm^{-1} , providing further support for the assignment of the 1024.2 and 939.8 cm^{-1} absorption bands to a $\text{C}_i\text{-O}_i\text{-Si}_i$ complex.

D. The vacancy-oxygen “A” center

In its neutral charge state, the well-known “A” center, the vacancy-oxygen center, produces optical absorption at 835.7 cm^{-1} . The measured isotope shift is -5.9 cm^{-1} , in close agreement with the *ab initio* prediction of -6.4 cm^{-1} using AIMPRO at Aveiro.¹⁴ The center is essentially a Si-O-Si complex with a substitutional oxygen atom distorted along a cube axis. The center has C_{2v} symmetry, and the observed infrared-active mode is the B_1 mode. AIMPRO predicts an A_1 mode to be almost resonant with the band states, at 565 cm^{-1} , and to have a ^{30}Si isotope shift of -18.0 cm^{-1} , very close to the value for an all-silicon mode. We have no data, since the A_1 mode has not been observed by infrared absorption and the “A” center is not photoluminescent, nor could we detect the very weak A_1+B_1 1370.0 cm^{-1} combination mode.³⁰

The AIMPRO calculations show that for the B_1 mode, 99% of the shift from $^{\text{nat}}\text{Si}$ to ^{30}Si originates from the two Si neighbors that are bonded to the oxygen atom. The next largest contribution is from the next Si atoms along the $\langle 110 \rangle$ chain (labeled “b” in Fig. 9 of Ref. 31), but each of these atoms only contributes 0.4% to the total shift. Consequently, an adequate vibrational model for the center is as a nonlinear symmetric Si-O-Si molecule, as used recently to describe Ge isotope effects for the vacancy-oxygen center in Ge.³² In this model, the vibrational frequency is

$$\omega_{B_1}^2 = k \frac{M_O + (2M_{\text{Si}})\sin^2 \alpha}{M_O M_{\text{Si}}}, \quad (1)$$

where M_O and M_{Si} are the masses of the O and neighboring Si atoms, k is a force constant, and 2α is the internal angle of the Si-O-Si chain. The oxygen isotope data (a shift of -37 cm^{-1} from ^{16}O to ^{18}O) may be fitted with $\alpha=80^\circ$, Ref. 33. Equation (1) then predicts that changing from ^{28}Si to ^{30}Si results in a frequency change by a factor of 0.992, compared to the measured 0.993.

IV. ELECTRONIC TRANSITIONS

The mid-infrared absorption of irradiated silicon often shows a strong line at 2767 cm^{-1} , which is produced by an internal electronic transition at the negative divacancy.³⁴ However, the line is more than an order of magnitude wider than is usual for a zero-phonon transition, and we will show that it has a *negative* isotope shift, in contrast to the shifts of all the zero-phonon lines reported to date.^{7,8} A broad line can occur when the transition being detected is not a zero-phonon line but is a vibronically induced transition. In this process, the optical transition from the ground state to an excited electronic state is forbidden, but it is made allowed if a phonon is created which can mix the electronic states of the center and make the transition allowed. A silver-related center in silicon is a recently discussed example of this process.³⁵ Changing the isotope would lower the frequency of the phonon, giving a negative isotope shift to the 2767 cm^{-1} line. The scientific and technological importance of the divacancy make it worth clarifying the nature of the optical transition. *Ab initio* theory is of no assistance in pre-

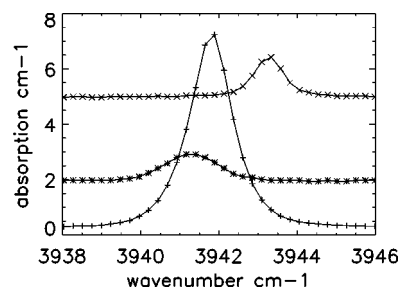


FIG. 2. Measured absorption produced by the 3942 cm^{-1} zero-phonon line in a $^{\text{nat}}\text{Si}$ sample doped with ^{12}C is shown by the line marked with + points, in $^{\text{nat}}\text{Si}$ doped with ^{13}C by the asterisks, and in ^{30}Si doped with ^{12}C by \times points. For clarity, the spectra have been displaced vertically.

dicting the isotope shifts of electronic transitions. We will therefore make use of an empirical method which has been used for zero-phonon lines of near-bandgap energy. The method is outlined in Sec. IV A, where we verify that it can also be applied to low-energy vibronic bands.

A. The 3942 cm^{-1} carbon-oxygen-vacancy center

The 3942 cm^{-1} vibronic band is generated in silicon by room temperature irradiation at doses sufficient to generate a second generation defect consisting of an interstitial-carbon atom and a vacancy trapped at an interstitial-oxygen atom.²⁶ The precise structure is not known. However, the optical properties of the center have been reported in detail, including the response of the zero-phonon line to strains and the temperature dependence of its energy.³⁶ There are no known local vibrational modes at the center. In Fig. 2 we now report that the $^{\text{nat}}\text{Si}$ to ^{30}Si isotope shift of the 3942 cm^{-1} line is significantly smaller, at $+1.5 \text{ cm}^{-1}$, than any previously measured zero-phonon line in silicon, which have all fallen in the range $+7$ to $+14 \text{ cm}^{-1}$, Refs. 7 and 8.

The effect of changing the isotopes on a zero-phonon line in silicon have been shown to come mainly from the difference in the vibrational frequencies in the ground and excited electronic states of the center.⁷ The same effects are also responsible for most of the change in energy of the zero-phonon line with temperature. Usually we expect that the vibrational modes will be softer in the excited state than in the ground state. The energy of the zero-phonon line then tends to higher energy as the effective mass increases, and to lower energy as the temperature increases. This expectation has been satisfied by all the zero-phonon lines whose isotope shifts have so far been measured in silicon.^{7,8}

For a quantitative discussion of the isotope effect we need to know the difference in vibrational frequencies in the ground and excited electronic states for all the lattice modes, which span the range 0 to 525 cm^{-1} . To extract this information from the measured temperature dependence of the zero-phonon energy requires data over a sufficient range of temperature that all the modes of vibration are sampled. It is not possible to detect a zero-phonon line in silicon at the high temperatures required—the Raman energy corresponds to 700 K , while zero-phonon lines are usually too broad and too weak to measure above 100 K . However, the indirect

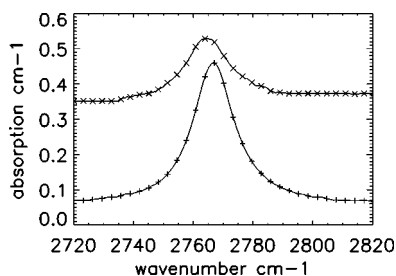


FIG. 3. Measured absorption produced by the divacancy in a ^{nat}Si sample doped with ^{13}C is shown by the line marked with + points, and in a ^{30}Si marked by \times points. For clarity, the ^{30}Si data have been displaced vertically and only representative datum points are shown.

energy gap has been measured over the necessary range.³⁷ For zero-phonon lines over 6000 cm^{-1} (relatively close to the band-gap energy) we have established an approximate rule that the temperature dependence of the indirect energy gap may be scaled to the temperature dependence of the zero-phonon line, over the range where it can be measured, to provide the information on the changes in vibrational frequency in the excited and ground states.⁷ This approach is now tested here on this much lower energy zero-phonon line.

Part of the temperature dependence of the energy of the 3942 cm^{-1} line comes from the lattice expansion (actually a contraction for silicon at low temperatures). Removing the contribution from the expansion effect, the difference in vibrational frequencies in the ground and excited electronic states produces a shift of -6 cm^{-1} from 0 to 100 K,³⁶ only 11% of the magnitude of the change in the indirect energy gap through the same process (Fig. 2 of Hayama *et al.*⁷). The vibrational term contributes $+17\text{ cm}^{-1}$ to the isotope shift of the energy gap; taking 11% of this produces an expected contribution to the shift of the 3942 cm^{-1} line of $+1.8\text{ cm}^{-1}$. Using the deformation potentials for the zero-phonon line,³⁶ the lattice contraction on changing the isotopes contributes a further $+1\text{ cm}^{-1}$ to the shift, giving a total predicted shift of $+2.8\text{ cm}^{-1}$. While this value is a factor of two greater than the experimental value of $+1.5\text{ cm}^{-1}$, it is very significantly smaller than is typical in silicon, in agreement with experiment. The simple scaling rule applies to the low energy 3942 cm^{-1} line.

B. The divacancy

The optical absorption at 2767 cm^{-1} (“ 0.34 eV ” or “ $3.6\text{ }\mu\text{m}$ ” line), produced by the singly negative charge state of the divacancy, is unexpectedly wide for a zero-phonon transition, at 16 cm^{-1} compared to the typical value of $\sim 1\text{ cm}^{-1}$. On isotopic substitution the line moves to *lower* energy, with a shift of -2.8 cm^{-1} , Fig. 3, in contrast to all the previously measured zero-phonon lines with their positive shifts (Hayama *et al.*^{7,8} and Sec. IV A). The sign would be consistent with a vibration being created in the transition. For example, an optic mode of 500 cm^{-1} would have an isotope shift of -16 cm^{-1} , and the effect on the optical transition would be reduced in magnitude by the typical positive shift, $\sim 10\text{ cm}^{-1}$, of the electronic transition.

To decide whether the 2767 cm^{-1} line is an anomalously broad zero-phonon line or a phonon-induced transition, we appeal to the scaling procedure used for the 3942 cm^{-1} line. The 2767 cm^{-1} line weakens and broadens considerably as the temperature increases,³⁴ moving by $+2\text{ cm}^{-1}$ up to 50 K. In this temperature range, the indirect energy gap moves by -15 cm^{-1} . Applying the scaling procedure leads to an estimated isotope shift for the 2767 cm^{-1} line produced by the electron-phonon term of -2.4 cm^{-1} . We have no data for the effect of the volume change on the energy of the line, but in all known cases it is smaller than the electron-phonon term. (Samaras³⁸ has measured the pressure dependence of some divacancy and vacancy-phosphorus levels, and the isotope-volume effect using those values would be $\sim \pm 1\text{ cm}^{-1}$). The similarity of the predicted and measured shifts suggests that the isotope effect on the 2767 cm^{-1} line can be explained in terms of its being an electronic transition, rather than involving a phonon. Since the line has only weak coupling to deformations of the lattice, as shown by its weak phonon sideband, the linewidth is unlikely to be caused by the local environmental strains. A linewidth of 16 cm^{-1} could occur through the lifetime broadening of $2 \times 10^{-12}\text{ s}$, which is plausibly longer than a typical vibrational period.

V. SUMMARY

We have reported on the effects of changing the lattice isotope on well-known vibrational absorption lines observed in silicon in the mid-infrared spectral range. We find an excellent agreement between the measured shifts of the vibrational frequencies in the ground electronic states of the centers and those predicted by density functional theory, Sec. III. The agreement, which depends on the correct predictions of the change in effective mass for each mode, strengthens the confidence in present-day *ab initio* theory.

A simple scaling rule, used to predict the isotope shifts of zero-phonon lines of much higher energy, has been shown to apply to the simple 3942 cm^{-1} zero-phonon line, Sec. IV A. The rule has been used to explain the unusual isotope shift of the 2767 cm^{-1} divacancy line, which, together with its large width, could suggest the involvement of a phonon in the transition. In Sec. IV B, the isotope shift has been shown to be consistent with the temperature dependence of the energy of the line, implying that it is indeed a simple zero-phonon transition, Sec. IV B. This does then raise the question of why it is so wide.

ACKNOWLEDGMENTS

The growth of samples was partly supported by a Grant-in-Aid for Scientific Research in Priority Area “Semiconductor Nanospintronics (No. 14076215).” The experimental work was supported by EPSRC grants No. (GR/R10820 and No. GR/R24531/01), by EU-INTAS Project No. 0268, and by a Study Visit to Aarhus University funded by the Royal Society of London. We thank Arne Nylandsted Larsen, Rui Pereira, and Knud Bonde Nielsen for assistance, Pia Bomholm Jensen for sample preparation, and P. Pavone for providing a data list of his one-phonon density of states.

*Electronic address: gordon.davies@kcl.ac.uk

- ¹T. Kojima, R. Nebashi, K. M. Itoh, and Y. Shiraki, *Appl. Phys. Lett.* **83**, 2318 (2003).
- ²D. Karaiskaj, M. L. W. Thewalt, T. Ruf, M. Cardona, and M. Konuma, *Solid State Commun.* **123**, 87 (2002).
- ³D. Karaiskaj, M. L. W. Thewalt, T. Ruff, and M. Cardona, *Phys. Status Solidi B* **235**, 63 (2003).
- ⁴D. Karaiskaj, G. Kirzenow, M. L. W. Thewalt, R. Buezko, and M. Cardona, *Phys. Rev. Lett.* **90**, 016404 (2003).
- ⁵D. Karaiskaj, T. A. Meyer, M. L. W. Thewalt, and M. Cardona, *Phys. Rev. B* **68**, 121201 (2003).
- ⁶D. Karaiskaj, J. A. H. Stitz, T. A. Meyer, M. L. W. Thewalt, and M. Cardona, *Phys. Rev. Lett.* **90**, 186402 (2003).
- ⁷S. Hayama, G. Davies, J. Tan, J. Coutinho, R. Jones, and K. Itoh, *Phys. Rev. B* **70**, 035202 (2004).
- ⁸S. Hayama, G. Davies, and K. M. Itoh, *J. Appl. Phys.* **96**, 1754 (2004).
- ⁹J. Kato, K. M. Itoh, H. Yamada-Kaneta, and H.-J. Pohl, *Phys. Rev. B* **68**, 035205 (2003).
- ¹⁰R. N. Pereira, T. Ohya, K. M. Itoh, and B. B. Nielsen, *Physica B* **340–342**, 697 (2003).
- ¹¹K. M. Itoh, J. Kato, M. Uemura, A. K. Kaliteevskii, O. N. Godisov, G. G. Devyatych, A. D. Bulanov, A. V. Gusev, I. D. Kovaliev, P. G. Sennikov, H. J. Pohl, N. V. Abrosimov, and H. Riemann, *Jpn. J. Appl. Phys., Part 1* **42**, 6248 (2003).
- ¹²*Annual Book of ASTM Standards, Procedure F123* (ASTM, Philadelphia, PA, 1992) ISBN 0-8031-1726-4, p. 189.
- ¹³J. M. Pruneda, S. K. Estreicher, J. Junquera, J. Ferrer, and P. Ordejon, *Phys. Rev. B* **65**, 075210 (2002).
- ¹⁴J. Coutinho, R. Jones, P. R. Briddon, S. Öberg, L. I. Murin, V. P. Markevitch, and J. L. Lindström, *Phys. Rev. B* **65**, 014109 (2001).
- ¹⁵H.-C. Wille, Y. V. Shvyd'ko, E. Gerdau, M. Lerche, M. Lucht, and H. D. Ruter, *Phys. Rev. Lett.* **89**, 285901 (2002).
- ¹⁶E. Sozontov, L. X. Cao, A. Kazimirov, V. Kohn, M. Konuma, M. Cardona, and J. Zegenhagen, *Phys. Rev. Lett.* **86**, 5329 (2001).
- ¹⁷C. H. Xu, C. Z. Wang, C. T. Chan, and K. M. Ho, *Phys. Rev. B* **43**, 5024 (1991).
- ¹⁸L. Hsu, M. D. McCluskey, and J. L. Lindström, *Phys. Rev. Lett.* **90**, 095505 (2003).
- ¹⁹J. L. McAfee and S. K. Estreicher, *Physica B* **340–342**, 637 (2003).
- ²⁰P. Giannozzi, S. Degironcoli, P. Pavone, and S. Baroni, *Phys. Rev. B* **43**, 7231 (1991).
- ²¹S. Hao, L. Kantorovich, and G. Davies, *Phys. Rev. B* **69**, 155204 (2004).
- ²²B. Pajot, E. Artachot, C. A. J. Ammerlaan, and J.-M. Spaeth, *J. Phys.: Condens. Matter* **7**, 7077 (1995).
- ²³A. R. Bean and R. C. Newman, *Solid State Commun.* **8**, 175 (1970).
- ²⁴L. I. Murin, V. P. Markevich, J. L. Lindström, M. Kleverman, J. Hermansson, T. Hallberg, and B. G. Svensson, *Solid State Phenom.* **82–84**, 105 (2002).
- ²⁵G. Davies and R. C. Newman, in *Carbon in Monocrystalline Silicon, Handbook on Semiconductors*, edited by S. Mahajan (North-Holland, Amsterdam, 1994), Vol. 3, p. 1557.
- ²⁶G. Davies, E. C. Lightowers, R. C. Newman, and A. S. Oates, *Semicond. Sci. Technol.* **2**, 624 (1987).
- ²⁷R. Jones and S. Öberg, *Phys. Rev. Lett.* **68**, 86 (1992).
- ²⁸G. Davies, A. S. Oates, R. C. Newman, R. Woolley, E. C. Lightowers, M. J. Binns, and J. G. Wilkes, *J. Phys. C* **19**, 841 (1986).
- ²⁹W. Kurner, R. Sauer, A. Dornen, and K. Thonke, *Phys. Rev. B* **39**, 13 327 (1989).
- ³⁰J. L. Lindström, L. Murin, V. Markevich, T. Hallberg, and B. Svensson, *Physica B* **273–274**, 291 (1999).
- ³¹V. Markevich, A. R. Peaker, J. Coutinho, R. Jones, V. J. B. Torres, S. Öberg, P. R. Briddon, L. I. Murin, L. Dobaczewski, and N. V. Abrosimov, *Phys. Rev. B* **69**, 125218 (2004).
- ³²P. Vanmeerbeek, P. Clauws, H. Vrielinck, B. Pajot, L. V. Hoo-rebeke, and A. N. Larsen, *Phys. Rev. B* **70**, 035203 (2004).
- ³³J. W. Corbett, G. D. Watkins, R. M. Chrenko, and R. S. McDonald, *Phys. Rev.* **121**, 1015 (1961).
- ³⁴J. H. Svensson, B. G. Svensson, and B. Monemar, *Phys. Rev. B* **38**, 4192 (1988).
- ³⁵G. Davies, T. Gregorkiewicz, M. Z. Iqbal, M. Kleverman, E. C. Lightowers, N. Q. Vinh, and M. X. Zhu, *Phys. Rev. B* **67**, 235111 (2003).
- ³⁶G. Davies, E. C. Lightowers, M. Stavola, K. Bergman, and B. Svensson, *Phys. Rev. B* **35**, 2755 (1987).
- ³⁷J. Hartung, L. A. Hansson, and J. Weber, in *Proc. 20th Int. Conf. on the Phys. of Semicond.*, edited by E. M. Anastassakis and J. D. Joannopoulos (World Scientific, Singapore, 1990), p. 1875.
- ³⁸G. A. Samara, *Phys. Rev. B* **39**, 12 764 (1989).